Monte Carlo studies of the magnetic phase diagram of $KEr(MoO_4)_2$: A dipolar magnet with strong tetragonal distortion

A. Orendáčová,[1] D. Horváth,[2] M. Orendáč,[1] E. Čižmár,[1] M. Kačmár,[1] V. Bondarenko,[3] A. G. Anders,[3] and A. Feher[1]
[1]*Department of Experimental Physics, P.J. Šafárik University, Park Angelinum 9, 041 541 Košice, Slovak Republic*
[2]*Department of Theoretical Physics and Geophysics, P.J. Šafárik University, Moyzesova 16, 040 01 Košice, Slovak Republic*
[3]*Institute of Low Temperature Physics and Engineering, Lenin Avenue 47, 310164 Kharkov, Ukraine*
(Received 27 March 2001; revised manuscript received 17 July 2001; published 4 December 2001)

The magnetic phase diagram of $KEr(MoO_4)_2$ a dipolar magnetic system with strong tetragonal distortion is investigated. The analysis of the experimental results indicates that the dipolar magnet with strong tetragonal distortion in external magnetic field applied along the easy axis resembles the behavior of the $S=1/2$ two-dimensional Ising model on the rectangular lattice in $B\|z$ with the nearest neighbor interactions only. The Monte Carlo studies of the corresponding critical B_c-T_c line revealed the second order character of the phase transitions down to the critical temperature ≈ 0.7 K and critical field $B_c \approx 50$ mT. The behavior of experimental and numerical data at lower critical temperatures suggests the vicinity of a tricritical point T_T characteristic for metamagnets.

DOI: 10.1103/PhysRevB.65.014420 PACS number(s): 75.30.Kz, 75.40.Mg, 75.10.−b

I. INTRODUCTION

The problem of the applicability of exchange coupling models for the description of magnetic structures with long-range interactions, especially for the systems with dominant dipolar interaction has been a subject of intensive theoretical and experimental investigations for a few decades. Materials such as dysprosium aluminum garnet (DAG) and $DyPO_4$ represent magnetic systems with dominant dipolar interactions which have cubic and weakly tetragonal ($c/a \approx 1$) lattices, respectively. It has been found that in zero magnetic field these high crystal symmetry materials may be approximated by the three-dimensional (3D) Ising model with the nearest-neighbor interaction.[1,2] The possibility of such approximation has been explained by the compensation of exchange and dipolar fields arising from the sites farther than the nearest neighbors. However, the exchange coupling models used in zero magnetic field analysis proved not to be useful for the description of the behavior observed in magnetic field. The experimental investigations have been completed by a number of mean-field studies of 3D antiferromagnetic Ising models with long-range interactions in external magnetic field[2,3] which approximate the studied materials.

The critical behavior of a dipolar Ising system on the simple tetragonal lattice with $c/a > 1$ has been theoretically studied in zero magnetic field.[4] It was revealed that the tetragonal dipolar lattice with the ratio $c/a > 2.5$ is in the universality class of the two-dimensional Ising model with short-range interactions. The conclusion was supported by Monte Carlo studies of 2D Ising antiferromagnet with long-range interactions in zero magnetic field.[5] Such behavior was experimentally observed in the rare earth (R) series of superconducting $RBa_2Cu_3O_{7-\delta}$ materials at low temperatures.[6–12] In these compounds the R subsystem forms nearly tetragonal lattice with $c/a \approx 3$ and $a/b \approx 1$. Since the $4f$ electrons of trivalent rare earths are effectively isolated from the superconducting (Cu-O) sublattice, magnetic correlations among R ions are predominantly of dipolar origin. Much less attention has been devoted to the investigation of the dipolar systems with a high c/a ratio in magnetic field B. Consequently, the present work attends to the experimental and numerical study of magnetic B-T phase diagram of the dipolar magnet with strong tetragonal distortion. The main motivation is to verify the applicability of the 2D Ising model with the nearest-neighbor interactions in the presence of external magnetic field applied parallel to the easy axis z. Generally, the behavior of the R magnetic subsystem in $RBa_2Cu_3O_{7-\delta}$ compounds was predominantly studied in the absence of the magnetic field because of the insufficient penetration of external magnetic field B into the superconducting specimen. The magnetic B-T phase diagrams of the R subsystem in nonsuperconducting $RBa_2Cu_3O_{7-\delta}$ series have been studied in detail.[13–16] However, the reduction of the oxygen content introduces significant changes in the effective magnetic lattice and spin dimensionality.[8–11]

Another class of dipolar magnets with the high c/a ratio is represented by the rare earth series with the general formula $AR(MoO_4)_2$, where A=Cs, K, Rb. The rare earth dimolybdates are ionic compounds with a layered crystal structure of orthorhombic symmetry[17] with nominally $a/c \approx 1$ and $b/a \approx 2$. Previous studies of a magnetic phase transition in zero magnetic field[18,19] together with the value of the latter ratio indicate that these dipolar systems approach theoretically predicted 2D behavior.

In particular, the present work is devoted to the experimental study of the temperature dependence of $KEr(MoO_4)_2$ specific heat in external magnetic field. On the basis of the specific heat data the experimental B-T phase diagram has been constructed. The analysis of the diagram was performed in the frame of two limit theories; a pure dipolar approach and the 2D Ising model with the nearest-neighbor coupling constants obtained from the previous $B=0$ analysis.[20] Since the exact solution for the $S=1/2$ 2D Ising model on the rectangular lattice in $B\|z$ is not known we have used mean-field approximation and the standard single-spin-flip Monte Carlo (MC) algorithm[21,22] to construct theoretical prediction for the B-T phase diagram of the 2D Ising model with the nearest-neighbor interaction.

The outline of the paper is as follows. Section II is devoted to the description of a sample and experimental apparatus used for the measurement of heat capacity. The construction and analysis of experimental and theoretical *B*-*T* diagram together with MC details is given in Sec. III. The main conclusions are summarized in Sec. IV.

II. EXPERIMENTAL DETAILS

The crystals of $KEr(MoO_4)_2$ have been prepared by the flux method[23] at the Institute of Low Temperature Physics in Kharkov. They were good optical quality crystals prepared in the shape of parallelepipeds with typical dimensions $15\times1\times10$ mm^3 with the edges cut along the a,b,c crystallographic axes. However, for the purposes of specific heat measurements in the vicinity of a phase transition much smaller piece of a sample was required to avoid the onset of extremely long relaxation times during the experiment. Because of the layered crystal structure, the materials preferably cleave in the ac plane. The optical quality of the crystal has been somewhat lowered due to crystallographic defects introduced by internal stressses during the cutting. A sample of approximate dimensions $6\times0.4\times3$ mm^3 and the weight of 33.6 mg was used for specific heat measurements. Since the crystal was not ellipsoidal in shape the fields inside the crystal were not uniform throughout, hence, strictly speaking there is no unique demagnetizing factor. Using the methods described in Refs. 24,25, the averaged value of $N\approx0.15$–0.2 was estimated for the used sample. The crystal was mounted in the experimental cell so that the applied field was parallel to the *c* axis. The specific heat measurements were performed using a dual slope method[26]—a relaxation technique established in the commercial ^{3}He-^{4}He dilution refrigerator TLE 200 type made by Oxford Instruments. The temperature of the sample was monitored by RuO_2 resistance thermometer manufactured by Dale Electronics with a nominal value of 1 kΩ, RC 550 type calibrated against a commercial germanium thermometer Lake Shore GR 200A-30. Magnetoresistive effects were not considered because of low values of applied magnetic field which did not exceed 130 mT, while the temperature in the measurement was not lower than 400 mK. The thermometer was varnished directly on the sample by GE 7031 varnish. For a homogeneous heating of the sample the tensometric gauge of nominal resistance 120 Ω was used varnished on the opposite side of the crystal. The entire assembly was suspended by nylon threads in the experimental cell and thermally connected to the thermal reservoir via a link made of silver wire of 50 μm diameter. No attention was paid to the addenda contribution since the specific heat was not directly analyzed and the temperatures of maxima necessary for the construction of *B*-*T* phase diagram could be obtained readily. Furthermore, our previous investigations show that the behavior of the addenda vs temperature is monotonous and in the vicinity of a phase transition does not exceed experimental inaccuracy of the used technique which is about 5%.

III. MAGNETIC PHASE DIAGRAM

$KEr(MoO_4)_2$ belongs to the most studied compounds from the aforementioned series. The crystal structure is orthorhombic with the symmetry D_{2h}^{14}, the parameters of the unit cell are $a=5.063$ Å, $b=18.25$ Å, and $c=7.915$ Å. However, the real distance between Er^{3+} ions along the *c* axis is $d=3.957$ Å. The unit cell contains two pairs of magnetically nonequivalent Er^{3+} ions with local symmetry axes tilted in the ac plane by the angle of $\pm9°$ with respect to the *c* axis. The ground state of a free Er^{3+} ion is $^4I_{15/2}$ with $2J+1$ degeneracy. This state is split by the local crystalline field into eight doublets with the lowest energies[27] $E_0=0$ and $E_1=15$ cm^{-1}. The energy separation $\Delta=E_1-E_0$ is much larger than Jahn-Teller interaction energy $A\approx4$ cm^{-1} estimated for $KEr(MoO_4)_2$. The condition $A<\Delta$ prevents the realization of the cooperative Jahn-Teller effect in the compound[28] in $B=0$ and magnetic fields sufficiently lower than the critical value $B_c\approx4$ T. In addition, electron paramagnetic resonance studies[28,29] performed at the temperatures from 1.8 to 4.2 K, revealed the field-induced Jahn-Teller effect only in *B* oriented perpendicular to the *c* axis for $B>4$ T. The Ising character of this compound at low temperatures is quite well established by a strong *g*-factor anisotropy with

$$g_a=1.8,\quad g_b<0.9,\quad g_c=g_\parallel=14.7, \tag{3.1}$$

corresponding to the lowest doublet. Given the tilting angle between the *c* axis and local symmetry axes is neglected, in the first approximation the *c* axis coincides with the easy axis *z* of the studied system. Previous thermodynamic studies of $KEr(MoO_4)_2$ in zero magnetic field[20] have revealed that below the temperature of about 5 K the system resembles the behavior of 2D $S=3/2$ Blume Capel model on a rectangular lattice. Below 2 K this model converges to the 2D $S=1/2$ Ising rectangular lattice model

$$\mathcal{H}_0=-J_1\sum_{i,j}\sigma_{i,j}^z\sigma_{i+1,j}^z-J_2\sum_{i,j}\sigma_{i,j}^z\sigma_{i,j+1}^z \tag{3.2}$$

with

$$\frac{J_1}{k_B}=0.85\ K,\quad \frac{J_2}{k_B}=-0.16\ K, \tag{3.3}$$

where J_1 represents effective intrachain exchange interaction and J_2 interchain interaction, σ_i^z takes on the values ±1. The magnetic phase transition into the antiferromagnetic ordered state has been observed at $T_N=0.955\pm0.005$ K. On the basis of the aforementioned facts the title compound might be an interesting subject of thermodynamic studies of magnetic phase diagram of Ising system with long-range interactions in $B\|z$.

A. Experimental data

The temperature dependence of $KEr(MoO_4)_2$ specific heat in constant magnetic field was studied in the temperature region under 1 K. Within the experimental accuracy the *c* axis of the crystal was aligned parallel to the magnetic field. For clarity, Fig. 1 only includes segments of the temperature dependence of the specific heat curves that contains the λ-like anomaly. It can be seen that the height of peaks

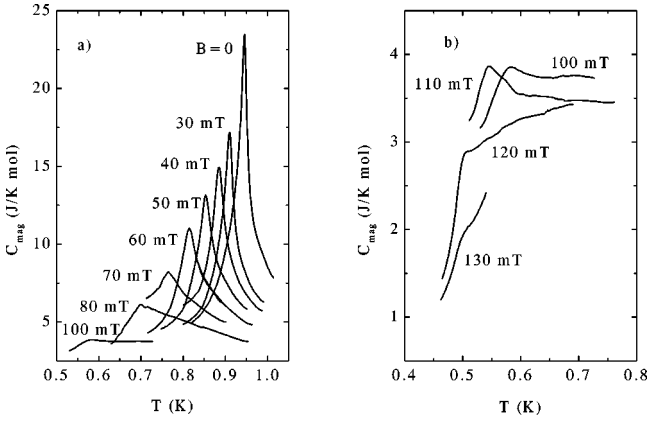

FIG. 1. (a),(b) The temperature dependence of $KEr(MoO_4)_2$ specific heat in constant external magnetic field $B\|c$.

steeply decreases with the increasing magnetic field while the width of the peaks increases. This behavior prevents any detection of a phase transition by specific heat measurements in magnetic fields higher than about 100 mT since the position of a maximum becomes practically unreadable. Taking the position of a maximum denoted as T_c observed in the corresponding magnetic field denoted as B_c, the magnetic phase diagram given in Fig. 2 has been constructed. It should be noted that in this experiment the temperature $T_N=0.946 \pm 0.005$ K is about 1% lower than the value observed in the previous experiment.[20] This difference can be explained by a combined effect of calibration error (the average relative error of the used thermometers is about 0.5%) and the crystallographic defects involved to the sample during the cutting of the material. The presence of the latter is indicated by the aforementioned lower optical quality of the crystal and the behavior of the specific heat in the vicinity of the phase

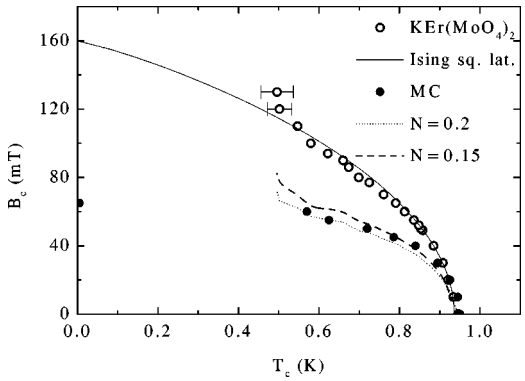

FIG. 2. Magnetic B-T phase diagram of $KEr(MoO_4)_2$ in external magnetic field $B\|c$ (open circles). The solid line represents the behavior of $S=1/2$ antiferromagnetic Ising model on the square lattice in $B\|z$. Magnetic B-T phase diagram of $KEr(MoO_4)_2$ corrected for demagnetizing effects for $N=0.15$ (dashed line) and $N=0.2$ (dotted line). For clarity the corrected data are presented by the lines drawn on the basis of the points shown in the Fig. 3. The full circles represent the MC prediction for $S=1/2$ Ising model on the rectangular lattice in $B\|z$ with $J_1/k_B=0.85$ K and $J_2/k_B=-0.16$ K. The estimated zero-temperature critical field $B_c^{0i(\mathrm{exch})}$ is also included.

transition; the maximal height of the peak is about 23 J/K mol which is lower in comparison with the value 30 J/K mol in the previous experiment. Furthermore, strong rounding appears; the width of the peak measured in the height 0.95 $C_{\max}$ is about 5 mK in the current experiment while the width of the peak in the previous experiment is about 1 mK. As was mentioned above, the current specific heat data did not enable the study of a low temperature part of the diagram. However, the zero-temperature value of B_c, denoted as B_c^0 provides information on the physical parameters of the system. Since our range of temperatures and magnetic fields is low in the comparison with Jahn-Teller interaction energy, we can neglect all types of spin-phonon and orbital-phonon interactions. Thus, as a further step B_c^0 was estimated by using the formula[30]

$$T_c = T_N\left[1-\left(\frac{B_c}{B_c^0}\right)^2\right]^{\xi}, \tag{3.4}$$

where $\xi=0.35$ for the Ising model on the simple cubic lattice and $\xi=0.87$ for Ising model on the square lattice with the nearest-neighbor interactions. Since the previous zero-field studies revealed the system resembles the behavior of two-dimensional Ising model under 2 K, the value $\xi=0.87$ was used in the fitting of the experimental phase diagram (Fig. 2). The fitting procedure yielded $B_c^0=160$ mT. Before the analysis of this value, the effect of a sample shape was considered. Assuming that the sample at zero temperature is fully magnetized in the paramagnetic region, saturated magnetization was calculated as $M_{\mathrm{sat}}=ng_{\|}\mu_B S$, where $n=5.48\times10^{27}$ atom/m^3 represents the number of Er atoms in the volume unit of the studied material, μ_B is Bohr magneton and $S=1/2$. Then internal magnetic field at zero temperature $B_c^{0i}=65$–90 mT was estimated by using the standard equation

$$B_c^{0i}=B_c^0-N\mu_0 M_{\mathrm{sat}}, \tag{3.5}$$

where μ_0 is the permeability of vacuum, the dependence of N on the position throughout the sample was replaced by the averaged value $N\approx0.15$–0.2. As shown in Ref. 31, given the magnetic correlations in the compound are predominantly of dipolar origin, the internal field B_c^{0i} can be directly related to the Zeeman energy $g_{\|}\mu_B B_c^{0i}$. This energy is required for the transition from the antiferromagnetic ground state with the corresponding energy E_A to the ferromagnetic ground state (saturated paramagnetic state) with the energy E_F

$$E_F-E_A=g_{\|}\mu_B B_c^{0i}. \tag{3.6}$$

The calculation of the energies performed within a pure dipolar approach[27] yielded $E_A/k_B=-1.3$ K and $E_F/k_B=-0.6$ K. In the latter the corrections for internal demagnetizing factor $N_0=1/3$ have been already included. The corresponding critical field resulting from Eq. (3.6) estimated in a pure dipolar approach is $B_c^{0i(\mathrm{dip})}=69.5$ mT. The reasonable agreement of the theoretical and experimental B_c^{0i} values indicates that the dipolar interactions play a dominant role in the magnetic subsystem of $KEr(MoO_4)_2$.

The 3D $S=1/2$ antiferromagnetic Ising model with exchange and dipolar interactions in magnetic field applied along the easy axis has been solved in the mean-field approximation yielding[2]

$$B_c^{0i}=\frac{2zJ}{g\mu_B}-\frac{1}{2}N_0M_{\rm sat}-B_{\rm dip}-B_{\rm exch}, \tag{3.7}$$

where J represents the total antiferromagnetic nearest-neighbor interaction-dipolar plus exchange, z represents the number of nearest neighbors, $B_{\rm dip}$ is the dipolar field arising from all ions on the opposite sublattice inside the sphere excluding the nearest neighbors in the paramagnetic state at $T=0$. Similarly $B_{\rm exch}$ is the exchange field arising from all ions on the opposite sublattice except the nearest neighbors. For $KEr(MoO_4)_2$ the value of B_c^{0i} obtained within the nearest-neighbor coupling calculation is $B_c^{0i(\rm exch)}=2zJ/g_\parallel\mu_B$, where $z=2$ and $J=J_2$, $J_2/k_B=-0.16$ K, yielding $B_c^{0i(\rm exch)}=64.7$ mT. The small difference in $B_c^{0i(\rm exch)}$ and $B_c^{0i(\rm dip)}$ indicates that the correspondence between the 2D Ising model with the nearest-neighbor interaction and dipolar magnet with strong tetragonal distortion is preserved also in the presence of external magnetic field $B\|z$.

To support this suggestion, the experimental data of the B-T diagram at finite temperatures corrected for the shape effects were analyzed in the frame of the 2D $S=1/2$ Ising model with the nearest-neighbor interaction

$$\mathcal{H}=\mathcal{H}_0-\frac{1}{2}g_\parallel\mu_BB\sum_i\sigma_i^z, \tag{3.8}$$

where $\mathcal{H}_0$ is introduced by Eq. (3.2) with the parameters given by Eqs. (3.1) and (3.3). The correction at finite temperatures has been performed using the relation

$$B_c^i=B_c-N\mu_0M(B_c^i,T_c), \tag{3.9}$$

where B_c^i denotes internal critical field at the temperature T_c. Since to our knowledge no experimental magnetization data are available, we used a simple approximation of M based on the assumption that the behavior of paramagnetic magnetization induced by the external magnetic field in the vicinity of a phase transition can be described by Brillouin function for $S=1/2$

$$M(B_c^i,T_c)=M_{\rm sat}\tanh\left(\frac{g_\parallel\mu_BB_c^i}{2k_BT_c}\right). \tag{3.10}$$

B_c^i is defined by Eq. (3.9). In a further step the corrected data given in Fig. 2 were analyzed in the frame of the aforementioned model.

B. Mean-field model

Mean field models can be considered as suitable starting points for the qualitative studies of the critical phenomena. For this step we proposed a simple version of the mean field approximation of the model (3.8) adapted from Ref. 32. The approach is based on the definition of the free energy density

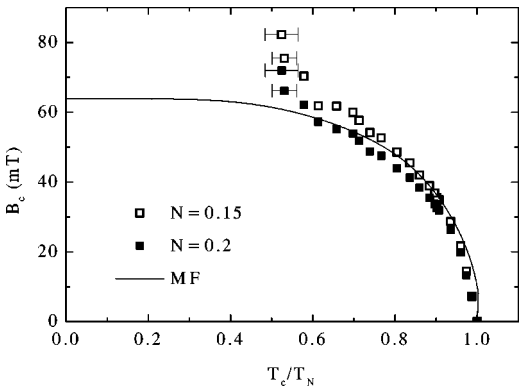

FIG. 3. Magnetic B-T phase diagram of $KEr(MoO_4)_2$ calculated in the mean-field approximation of the model (3.8) (solid line). The open and full squares represent experimental data corrected for demagnetizing effects with $N=0.15$ and 0.2, respectively.

$$F=-J_1(m_1^2+m_2^2)-2J_2m_1m_2-\frac{1}{2}g_\parallel\mu_BB(m_1+m_2)$$
$$+\frac{1}{2}k_BT[(1+m_1)\ln(1+m_1)+(1-m_1)\ln(1-m_1)$$
$$+(1+m_2)\ln(1+m_2)+(1-m_2)\ln(1-m_2)], \tag{3.11}$$

where m_1, m_2 are sublattice site magnetizations. The total magnetization per site is defined as $m=(1/2)(m_1+m_2)=M/M_{\rm sat}$. Having applied the conditions for the existence of the extreme of F, $\partial F/\partial m_1=\partial F/\partial m_2=0$ we obtained the equations

$$m_1=\tanh(j_1m_1+j_2m_2+h), \tag{3.12}$$

$$m_2=\tanh(j_1m_2+j_2m_1+h), \tag{3.13}$$

where $j_1=(2J_1)/(k_BT)$, $j_2=(2J_2)/(k_BT)$ and $h=(g_\parallel\mu_BB)/(4k_BT)$. This system of equations was solved numerically for the parameters (3.1), (3.3) and the stable solution corresponding to the minimum of the free energy has been selected. The solution consists of paramagnetic and antiferromagnetic branches corresponding to the jump of the total magnetization M_c on the critical B_c-T_c line presented in Fig. 3. The calculation confirms that $B_c^{0(\rm MF)}=B_c^{0i(\rm exch)}$, while the zero-field critical temperature is approximately twice larger than T_N observed in the experiment. This difference in the temperatures can be considered as a typical artifact of the used mean-field approach. The magnetization jump on the critical line indicates that the system exhibits the first order phase transition in the full temperature range. However, experimental study of the specific heat performed in a wide temperature interval did not reveal the existence of two peaks characteristic for a mixed phase present under the tricritical temperature. As can be seen from Fig. 3, qualitatively good agreement between the theory and experimental data corrected for demagnetizing effects has been achieved down to $T_c/T_N\approx0.6$. The question whether the character of the phase transition really coincides with the prediction of the mean-field calculation has been the main subject of our Monte Carlo studies.

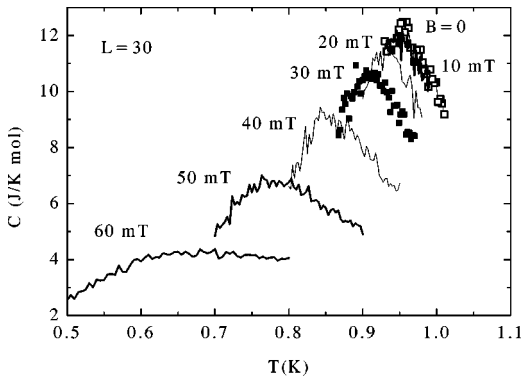

FIG. 4. MC simulations of the temperature dependence of specific heat of $S=1/2$ Ising model on the rectangular lattice with $J_1/k_B=0.85$ K and $J_2/k_B=-0.16$ K in $B\|z$.

C. Monte Carlo results

Monte Carlo (MC) single spin flip calculations have been applied to perform a detailed analysis of the model (3.8) with the parameters given by Eqs. (3.1),(3.3). The physical quantity of the main interest is the specific heat calculated by using the fluctuation-dissipation formula

$$C=R\frac{\langle E^2\rangle-\langle E\rangle^2}{(k_BT)^2L^2}, \tag{3.14}$$

where $\langle\cdots\rangle$ means the ensemble average, $\langle E\rangle$ is the mean energy of a lattice consisting of $L\times L$ spins, and R is the gas constant. The MC simulations were carried out for periodic boundary conditions, various size lattices, from $L=10$ up to $L=50$ and for various numbers of MC steps. The MC simulation on the larger of the lattices comprised 5×10^4 initialization steps/spin to equilibrate the system. Consequently, 3×10^5 steps/spin were done to calculate the statistical averages of interest. The MC simulations of the equilibrium temperature dependences were performed by starting at $T>T_c$ from a randomly chosen spin configuration close to the paramagnetic state. Then the magnetic field was switched on and the system was cooled with a temperature step ΔT in a field-cooling regime in the same way as the experimental measurements. The MC calculations of the temperature dependence of specific heat in the constant magnetic field revealed the presence of a phase transition from the paramagnetic into the antiferromagnetically ordered state at the temperatures approaching the value of the pseudocritical temperature $T_c(L)$. The magnetic field varied from 0 to 60 mT. The extreme rounding of specific heat maximum observed in the fields above 60 mT prevented us from further calculations in higher magnetic fields (Fig. 4). The resulting points of the B_c-T_c line were constructed in the similar way like the experimental diagram by taking the position of the specific heat maximum and the corresponding magnetic field. The maximum $C_{\max}(L)$ and the position of the maximum $T_c(L)$ were obtained as parameters of the fitting procedure performed in the critical region where the specific heat was approximated by the phenomenological formula

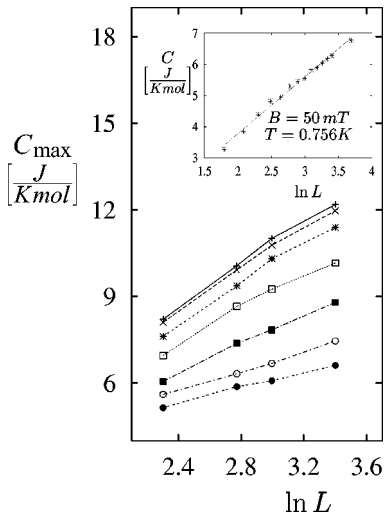

FIG. 5. The finite size dependence of a specific heat maximum $C_{\max}(L)$ in the magnetic field $B=0$ (plus), 10 mT (cross), 20 mT (asterisk), 30 mT (open square), 40 mT (full square), 45 mT (open circle), 50 mT (full circle). The inset shows that the specific heat calculated for $B=50$ mT at $T=0.756$ K taken from the neighborhood of T_c and $L=8$–40 is also logarithmic with respect to L.

$$C(L,T)=C_{\max}(L)-\left(\frac{T-T_c(L)}{\Delta(L)}\right)^2 \tag{3.15}$$

reflecting the rounding effects. The strength of the rounding is characterized by the parameter $\Delta(L)$. The fitting was repeated iteratively within the temperature range $\langle T_c(L)-\Delta(L),T_c(L)+\Delta(L)\rangle$ until the variations of the fitted $T_c(L)$, $\Delta(L)$, and $C_{\max}(L)$ reached a fixed point.

The dependence $C_{\max}(L)$ vs L is the signature of the character of a phase transition; the second order phase transition leads to the logarithmic behavior $C_{\max}(L)\propto\ln L$ whereas quadratic dependence $C_{\max}(L)$ should indicate the presence of the first order transition.[22] The logarithmic plot in Fig. 5 indicates that the transition is of the second order for $B<50$ mT. The behavior of $C_{\max}(L)$ for larger field values is not transparent due to prevailing statistical errors. The MC calculations performed for various L revealed significant finite size effects including the shift of $T_c(L)$ towards lower values with increasing L. In the following, finite size scaling of $T_c(L)$ was performed to obtain the estimation of the phase diagram for the infinite system. The analysis of $C_{\max}(L)$ vs L dependence suggests that at least for the lower fields the extrapolation

$$T_c(L)=T_c+b/L \tag{3.16}$$

is justified. This formula involves two unknown parameters: the true critical temperature T_c and thermal coefficient b, which is the measure of the shift of the critical temperature for the finite system. However, the fitting of $T_c(L)$ can provide rather naive prediction if the number of lattices is small. To avoid this problem, we have supplemented the scaling technique [Eq. (3.16)] by the method in which the plot $C(L,T)$ vs $L(T-T_c)$ is used for the location of the true T_c; finding this value requires that the specific heat peaks coincide near the critical region (Fig. 6).

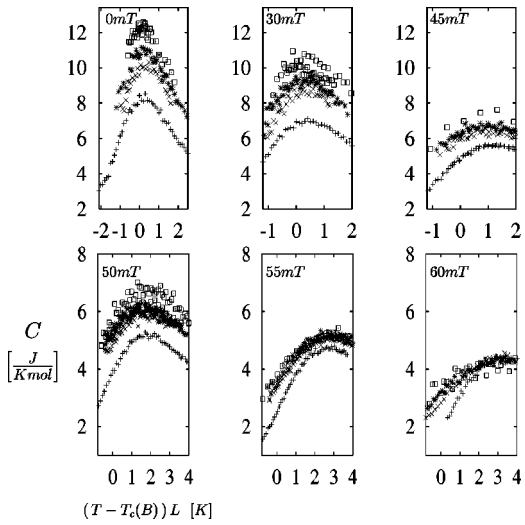

FIG. 6. Specific heat vs scaled temperature $[T-T_c(B)]L$ in constant magnetic field calculated for various lattices $L=10$ (plus), $L=16$ (cross), $L=20$ (asterisks), and $L=30$ (dot square).

Another subsidiary tool for the analysis of the position of critical points is Binder's cumulant technique.[22] In the case of the antiferromagnetic chainlike system, the suitable form of Binder's cumulant is

$$U_M = 1 - \frac{\langle M_{\rm st}^4 \rangle}{3\langle M_{\rm st}^2 \rangle^2}, \tag{3.17}$$

where $M_{\rm st}$ is the staggered magnetization defined as an absolute value of the difference of sublattice magnetizations in two adjacent chains along the c axis. In the case of the second order phase transition $U_M(L,T)$ is invariant under the change of L for T approaching T_c (Fig. 7). The application of Binder's cumulant technique requires the special care in the interpretation of the cumulant crossings constructed for different lattices. The treatment of U_M also requires better statistics of the data compared to the statistics necessary for the specific heat. It was found that a regular behavior of $U_M(L,T)$ providing reasonable predictions comparable with the predictions from the specific heat requires the calculation of averages over 10^6 MC steps/site.

Using the estimation of T_c obtained by Binder's cumulant technique, the second order character of the phase transition in $B=50$ mT has been verified; a temperature T from a critical region around the T_c has been chosen and the behavior of $C(T,L)$ vs $\ln L$ dependence has been investigated. The good linearity of the dependence clearly indicates the second order character of the phase transition[22] [Fig. 5 (inset)].

The significant contradictions between the estimations of T_c yielded by Binder's cumulant technique and the previous two methods were observed for $B=60$ mT. A complicated crossing of the Binder's cumulants appears close to the value $T_c=0.45$ K, whereas rescaling of the specific heat provides $T_c=0.55$ K. In the case $B=60$ mT, the rounding of specific heat peaks attains the resolution threshold. Thus, we tried to analyze the numerical data by using the energy cumulant method based on the definition of the quantity[22]

$$V_E = 1 - \frac{\langle E^4 \rangle}{3\langle E^2 \rangle^2}. \tag{3.18}$$

Contrary to our expectation of some anomaly, also in the worst case $B=60$ mT the careful analysis of V_E in the vicinity of the aforementioned $T_c=0.45$ K shows only small deviations of the order of 10^{-7} from the limiting value 2/3 typical for the second order phase transition. The coincidence is better for larger lattices (Fig. 7).

In the following we attend to the investigation of the formal resemblance between the specific heat maxima determined experimentally and by Monte Carlo technique. As was mentioned above the width of the peaks is proportional to $\Delta(L)$. In the case of the second order transition one can write $\Delta(L)=c_0/L$, where c_0 is the universal constant independent of the lattice size. The parameter c_0 was chosen here as a useful measure of the rounding effects of the Monte Carlo specific heat data. The comparison of c_0 and b indicates that rounding and shifting effects are of the same order in the amplitude and increase with increasing magnetic field. The comparison of these quantities with the width of the experimental peaks W_p defined as the one at which the value of specific heat is 95% of its maximal value $C_{\rm max}$ (see Fig. 8) shows the qualitative agreement. This similar behavior of the Monte Carlo and experimental results is probably associated with the aspect of the finite size effects in the former while in the latter it corresponds to the combined influence of crystal lattice defects due to the space distribution of local easy axes and nonellipsoidal sample shape effects. The broadening pronounced in external magnetic fields higher than about 70 mT and critical temperatures under 0.75 K (Fig. 8) indirectly indicates that the system might be in a domain state, i.e., in these external fields the system with $N\neq 0$ achieves so called mixed phase consisting of antiferromagnetic and paramagnetic domains. According to Eq. (3.9), the external field 70 mT corresponds to the internal field $B^i \approx 45$–50 mT which

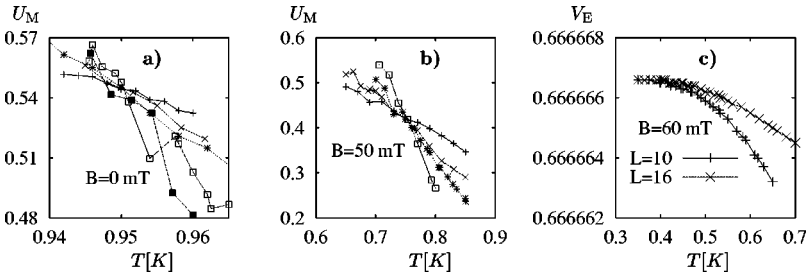

FIG. 7. (a) The temperature dependence of Binder's cumulant in $B=0$ for various lattices: $L=10$ (plus), $L=16$ (cross), $L=20$ (asterisk), $L=30$ (dot square), $L=40$ (full square). (b) The temperature dependence of Binder's cumulant in $B=50$ mT for various lattices: $L=10$ (plus), $L=16$ (cross), $L=20$ (asterisk), $L=30$ (dot square). (c) The temperature dependence of the energy cumulant in $B=60$ mT for various lattices.

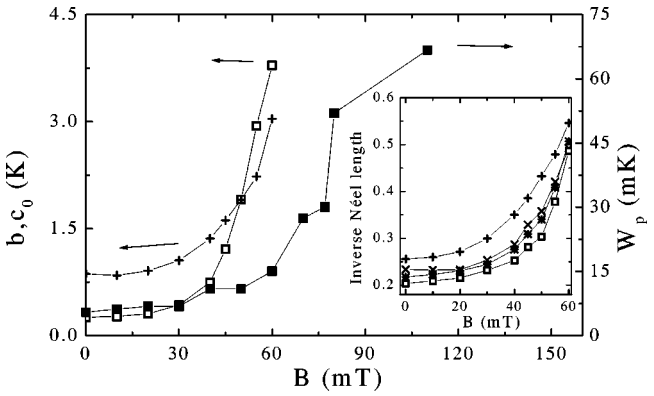

FIG. 8. Magnetic field dependence of the shifting parameter b (open square) and rounding parameter c_0 (plus). External magnetic field dependence of the width of the peak in the experimental specific heat of $KEr(MoO_4)_2$ (full square). The inset shows magnetic field dependence of the inverse Néel length calculated at $T_c(L)$ for various lattices $L=10$ (plus), $L=16$ (cross), $L=20$ (asterisk), and $L=30$ (open square).

might indicate the vicinity of a tricritical point. This suggestion is supported by isothermic measurement of $KEr(MoO_4)_2$ magnetization at $T=0.6$ K in $B\|c$, where a metamagnetic phase transition has been observed[33] with the rough approximation of the critical fields $B_{\rm low}\approx 70$ mT and $B_{\rm high}\approx 200$ mT. The used temperature is rather low, so we can assume $B_{\rm low}\approx B_c^{0i}$. Since the authors in Ref. 33 did not perform any correction for demagnetizing effects, we cannot quantitatively compare their results with our MC predictions.

We now address the question how the rounding and shifting are related to the corresponding spin configuration. We found that appropriate quantity proportional to the cross section of 2D spin clusters of the studied antiferromagnetic chainlike system is the Néel length l_n introduced by the expression

$$l_n = L^2\left(L + \left\langle \sum_{i,j=1}^{L\times L} \delta_{\sigma^z_{i,j},\sigma^z_{i,j+1}} \right\rangle \right)^{-1}, \qquad (3.19)$$

where the terms with the usual Kronecker's delta function sum up the number of pairs of neighboring spins with the same projection; the pairs break the antiferromagnetic order in the direction perpendicular to the c axis. The temperature dependence $l_n(T)$ was calculated for various fields and various lattice sizes. The rapid decrease of the quantity with the increasing field observed on the critical B_c–$T_c(L)$ line above 50 mT indicates the growth of paramagnetic clusters [Fig. 8 (inset)]. Such development of spin structure corresponds to the similar behavior of the rounding and shifting effects with respect to the magnetic field.

IV. SUMMARY AND CONCLUSIONS

Experimental study of the magnetic phase diagram of $KEr(MoO_4)_2$ single crystal has been performed by the method of specific heat measurements in constant external magnetic field applied along the easy axis. The obtained experimental data were corrected for the demagnetizing effects. The analysis of the experimental and theoretical zero-temperature value of the critical field B_c^{0i} suggests the preservation of the correspondence between the 2D Ising model with the nearest-neighbor interaction and dipolar magnet with strong tetragonal distortion even in the presence of the magnetic field applied along the easy axis. This conjecture has been supported by the analysis of the experimental phase diagram performed in the frame of the 2D Ising model with the nearest-neighbor interactions. Theoretical studies of this model using the mean-field approximation yield the prediction for the B-T phase diagram which qualitatively describes the behavior of experimental data in lower magnetic fields. Monte Carlo calculations have been applied to elucidate the order of the phase transitions on the critical B_c-T_c line. The MC finite size scaling analysis unambiguously confirms the second order character of the B_c-T_c line at least up to the fields of 50 mT. The steep increase of the b,c_0 parameters and the inverse Néel length in higher fields together with rising statistical errors coincides with the steep increase of the width of experimental specific heat peaks. This behavior might indicate the vicinity of a tricritical point. Consequently, the classical single-spin flip algorithm dynamics becomes extremely slow and not very effective even for smaller lattices where the corrections to the scaling may be of considerable importance.[34,35] In this region critical exponents are affected, hence, MC studies of crossover phenomena yield less reliable results.[36] Furthermore, as is demonstrated in the current work, the ignoring of the potential existence of the first order character of the critical line can be a source of disagreement between the estimations of true critical temperatures yielded by different methods.

As was shown in Refs. 37,38 the algorithm working with spin cluster flips[39] or loops is more effective than the single spin flip algorithm in the recovering of the first order line at low temperatures. We suppose that completion of the whole theoretical phase diagram of $KEr(MoO_4)_2$ will require the application of such efficient MC methods. As for the experimental counterpart, the extension of the diagram down to lower temperatures could be performed by experimental measurements of isothermic magnetization carried out on a sample with a well defined demagnetizing factor. We expect that this complex study might support the suggestion that the critical behavior of tetragonal dipolar magnet in the field parallel to the easy axis resembles the behavior of 2D metamagnet with the nearest-neighbor interactions. Similar features have been observed in the MC studies of Ising dynamics in dots of patterned magnetic materials in external magnetic field. The studies led to the conclusion that the involving of a long-range magnetic interaction of the type $N(M/M_{\rm sat})^2$ into short-range Ising system does not bring a significant change in Monte Carlo relaxation dynamics.[40]

ACKNOWLEDGMENTS

This work was supported in part by NSF Grant No. INT-0089140 and Slovak Ministry of Education Grant Nos. 1/7473/20 and 1/6020/99. The material support of U.S. Steel DZ Energetika is gratefully acknowledged.

[1] D. P. Landau, B. E. Keen, B. Schneider, and W. P. Wolf, Phys. Rev. B **3**, 2310 (1971).
[2] C. S. Koonce, B. W. Mangum, and D. D. Thornton, Phys. Rev. B **4**, 4054 (1971).
[3] J. C. Wright, H. W. Moos, J. H. Colwell, B. W. Mangum, and D. D. Thornton, Phys. Rev. B **3**, 843 (1971).
[4] K. De'Bell and J. P. Whitehead, J. Phys.: Condens. Matter **3**, 2431 (1991), and references therein.
[5] A. B. MacIsaac, J. P. Whitehead, K. De'Bell, and K. Sowmya Narayanan, Phys. Rev. B **46**, 6387 (1992).
[6] S. Simizu, S. A. Friedberg, E. A. Hayri, and M. Greenblatt, Phys. Rev. B **36**, 7129 (1987).
[7] J. W. Lynn, T. W. Clinton, W.-H. Li, R. W. Erwin, J. Z. Liu, K. Vandervoort, and R. N. Shelton, Phys. Rev. Lett. **63**, 2606 (1989).
[8] T. W. Clinton, J. W. Lynn, J. Z. Liu, Y. X. Jia, T. J. Goodwin, R. N. Shelton, B. W. Lee, M. Buchgeister, M. B. Maple, and J. L. Peng, Phys. Rev. B **51**, 15 429 (1995).
[9] Y. Nakazawa, M. Ishikawa, and T. Takabatake, Physica B **148**, 404 (1987).
[10] K. N. Yang, J. M. Ferreira, B. W. Lee, M. B. Maple, W.-H. Li, J. W. Lynn, and R. W. Erwin, Phys. Rev. B **40**, 10 963 (1989), and references therein.
[11] T. Chattopadhyay, H. Maletta, W. Wirges, K. Fischer, and P. J. Brown, Phys. Rev. B **38**, 838 (1988).
[12] J. W. Lynn, W.-H. Li, Q. Li, H. C. Ku, H. D. Yang, and R. N. Shelton, Phys. Rev. B **36**, 2374 (1987).
[13] V. P. Dyakonov, E. E. Zubov, L. P. Kozeeva, G. G. Levchenko, V. I. Markovich, A. D. Pavlyuk, and I. M. Fita, Physica C **178**, 221 (1991).
[14] A. I. Zvyagin, A. A. Stepanov, E. N. Khatsko, A. S. Cherny, V. I. Dotsenko, and N. M. Chaikovskaya, Fiz. Nizk. Temp. **16**, 665 (1990).
[15] I. M. Fita, V. P. Dyakonov, G. G. Levchenko, V. I. Markovich, and L. P. Kozeeva, Phys. Solid State **36**, 1892 (1994).
[16] V. P. Dyakonov, E. E. Zubov, L. P. Kozeeva, G. G. Levchenko, V. I. Markovich, A. A. Pavlyuk, and I. M. Fita, Sov. Phys. Solid State **34**, 278 (1992).
[17] In the coordinate system usually used in the structural studies of rare earth dimolybdates *b* and *c* axes correspond to the *c* and *b* axes, respectively, used in the aforementioned theoretical works.
[18] P. Stefanyi, A. Feher, A. Orendáčová, E. E. Anders, and A. I. Zvyagin, J. Phys. (France) **50**, 1297 (1989).
[19] P. Stefanyi, A. Feher, and A. Orendáčová, J. Phys.: Condens. Matter **1**, 7529 (1989).
[20] D. Horváth, A. Orendáčová, M. Orendáč, M. Jaščur, B. Brutovský, and A. Feher, Phys. Rev. B **60**, 1167 (1999), and references therein.
[21] C. Domb and M. S. Green, *Phase Transitions and Critical Phenomena* (Academic Press, London, 1976), Vol. 5b; S. Wansleben and D. P. Landau, Phys. Rev. B **43**, 6006 (1990).
[22] K. Binder, *Monte Carlo Methods in Statistical Physics* (Springer, Berlin, 1979).
[23] V. A. Vinokurov and P. V. Klevtsov, Kristallografiya **17**, 127 (1972).
[24] R. I. Joseph and E. Schlomann, J. Appl. Phys. **36**, 1579 (1965).
[25] D. J. Craik, *Structure and Properties of Magnetic Materials* (Pion Limited, London, 1971).
[26] S. Riegel and G. Weber, J. Phys. E **19**, 790 (1986).
[27] A. G. Anders, S. V. Volotskii, and O. E. Zubkov, Fiz. Nizk. Temp. **20**, 131 (1994).
[28] V. I. Kutko, M. I. Kobets, B. A. Pashchenko, and E. N. Khatsko, Fiz. Nizk. Temp. **21**, 441 (1995).
[29] V. I. Kutko and M. I. Kobets, Fiz. Nizk. Temp. **21**, 1169 (1995).
[30] A. Bienenstock, J. Appl. Phys. **37**, 1459 (1966).
[31] A. G. Anders, S. V. Volotskii, and O. E. Zubkov, Fiz. Nizk. Temp. **20**, 137 (1994).
[32] H. Yoshizawa and D. P. Belanger, Phys. Rev. B **30**, 5220 (1984).
[33] E. N. Khatsko, A. S. Cherny, and A. I. Kaplienko, Fiz. Nizk. Temp. **19**, 1217 (1993).
[34] L. Hernandez and H. T. Diep, Phys. Rev. B **55**, 14 080 (1997).
[35] A. K. Jain and D. P. Landau, Phys. Rev. B **22**, 445 (1980).
[36] K. Binder and E. Luijten, Comput. Phys. Commun. **127**, 126 (2000).
[37] A. Hucht and K. D. Usadel, J. Magn. Magn. Mater. **156**, 423 (1996).
[38] R. G. Melko, B. C. den Hertog, and M. J. P. Gingras, Phys. Rev. Lett. **87**, 067203 (2001).
[39] R. H. Swendsen and J. S. Wang, Phys. Rev. Lett. **58**, 86 (1987).
[40] P. A. Rikvold, M. A. Novotny, M. Kolesik, and H. L. Richards (unpublished).